NASA CR-
80023

DEVELOPMENT OF AN

INFINITE-INPUT-IMPEDANCE FLUIDIC AMPLIFIER

By E. Martinez

June 1967

Prepared under Contract No. NAS 12-43
Astromechanics Research Division
Giannini Controls Group
CONRAC CORPORATION
Malvern, Pennsylvania

Electronics Research Center
NATIONAL AERONAUTICS AND SPACE ADMINISTRATION

NASA CR-

DEVELOPMENT OF AN INFINITE-INPUT-IMPEDANCE FLUIDIC AMPLIFIER

By E. Martinez

June 1967

Prepared under Contract No. NAS 12-43

Astromechanics Research Division
Giannini Controls Group
CONRAC CORPORATION
Malvern, Pennsylvania

Electronics Research Center
NATIONAL AERONAUTICS AND SPACE ADMINISTRATION

TABLE OF CONTENTS

LIST OF FIGURES

NOMENCLATURE

a	Cross-sectional area of needle
A	Cross-sectional area of chamber
c	Damping coefficient
C_c	Control capacitance
C_o	Output capacitance
F_f	Friction force
F_1	Force acting on bead - control side
F_2	Force acting on bead - needle side
G	Pressure Gain
K	Effective gas spring constant
K_1, K_2, k	Constants
ℓ	Length of bead
M	Mass of bead
n	radius at which $p = .37p_n$/needle radius
p_c	Control pressure
p_s	Supply pressure
p_o	Output pressure
p_{ch}	Chamber pressure
p_n	Pressure at tip of needle
p_b	Pressure on bead
p_{st}	Static pressure
p_d	Dynamic pressure
R_n	Needle resistance
R_s	Supply resistor
R_v	Variable resistance caused by bead movement

R_o	Output resistor in buffer-gain unit
R	Radius of bead cross section
R_c	Control resistor
r_n	Variable radius
S	Bead surface projection normal to chamber axis
s	Laplace transform variable
T_o	Time constant - output circuit
T_i	Time constant - input circuit
v	Gas velocity
x	Position co-ordinate
x_o	Length of air space
ω	Frequency
ω_n	Bead natural frequency
γ	Ratio of specific heats
ρ	Density
P, P_o, P_c, P_c', X	Laplace transform of the corresponding variables
ξ	Damping factor

DEVELOPMENT OF AN INFINITE-INPUT-IMPEDANCE FLUIDIC AMPLIFIER

By E. Martinez

Conrac Corporation
Astromechanics Research Division
Malvern, Pennsylvania

SUMMARY

This report describes the analytical and experimental work carried out during the development of two-phase analog fluidic amplifiers, for infinite input impedance and highly stable gains. Three basic configurations were studied in detail: a buffer (one-to-one) amplifier, a gain amplifier, and a buffer-gain amplifier (which is a variation of the buffer configuration with high gain). In addition, an exploratory chemical investigation was performed to evaluate non-toxic chemical systems to replace the mercury used in the original units. It was found that friction produced significant hysteretic effects in the gain-type amplifier, but had no apparent effect on the other two configurations. The buffer and buffer-gain amplifiers exhibit good linearity. Frequency response experiments on these units showed them to have a bandwidth in excess of 50 hertz. The performance of these two devices is more than adequate for use in many fluidic operational amplifier circuits.

INTRODUCTION

The technology of fluidic systems is expanding at an ever increasing rate. A great deal of the groundwork has already been done and there is a modest, but increasing, availability of fluidic components. We see, every day, a growing number of fluidic computers and control systems, both at the prototype stage and as operational hardware. However, it is in these applications that we encounter limitations as to the computational capabilities of fluidic amplifiers. Accurate integration and differentiation operations, intrinsic to computation and system compensation, have been handicapped by the lack of stable, high-gain, high-input-impedance amplifiers. Alternate methods, such as "bootstrap" integration, demand prohibitive performance of the components for accurate computation.

The two-phase fluidics concept developed for use in the Conrac non-destructive memory units has been extended to provide a solution to this problem. This concept makes use of two different fluids in the same device, one of which is restrained inside by its own surface tension. Thus we effectively have the fluid equivalent of a low-spring-constant flexible diaphragm. With this element, it is possible,first, to separate the control and output circuits so no control flow is required (infinite input

impedance), and second, to construct a force-balance device in which the gain is only a function of some invariant physical parameters of the unit (stable gain).

This report describes the development of various two-phase fluidic amplifiers, as well as the static and dynamic characteristics of final prototypes. The results of this phase of the development are in the form of amplifier designs optimized for functional performance.

The author wishes to acknowledge the contributions of Conrac Corporation personnel to the success of the program reported in this document: N. G. Barr in analysis and design, J. Flear in the fabrication of hardware, B. Pahl and T. Shaffer in experimental testing and data reduction, and R. Jacksteit in the preparation of this report.

THEORETICAL ANALYSIS

Static Analysis

The static characteristics of the infinite-input-impedance units depend on the bead force balance as well as on the relative values of the resistances in the circuit.

The force-balance equation and the circuit equations are solved simultaneously to obtain the output pressure as a function of the control pressure and other parameters. Finally, the gain equation is obtained by taking the derivative of the output pressure with respect to the control pressure. The details of the derivations will now be covered for the three configurations shown in Figure 1.

Buffer (one-to-one) amplifier.--The circuit equation (from Figure 1(a)) is:

$$\frac{p_s}{R_s + R_v + R_n} = \frac{p_o}{R_v + R_n} \tag{1}$$

Solving for p_o and rearranging the equation, we have:

$$p_o = \left\{ \frac{1}{\frac{R_s}{R_n + R_v} + 1} \right\} p_s \tag{2}$$

When the bead is far from the needle exit, R_v approaches zero. Then:

$$p_o \Big|_{R_v \to 0} = \left\{ \frac{1}{\frac{R_s}{R_n} + 1} \right\} p_s \tag{3}$$

Under complete shut-off, i.e. when R_v approaches infinity, we have:

$$p_o \Big|_{R_v \to \infty} = p_s \tag{4}$$

Equations (3) and (4) define the pressure output at both extremes of the operating range.

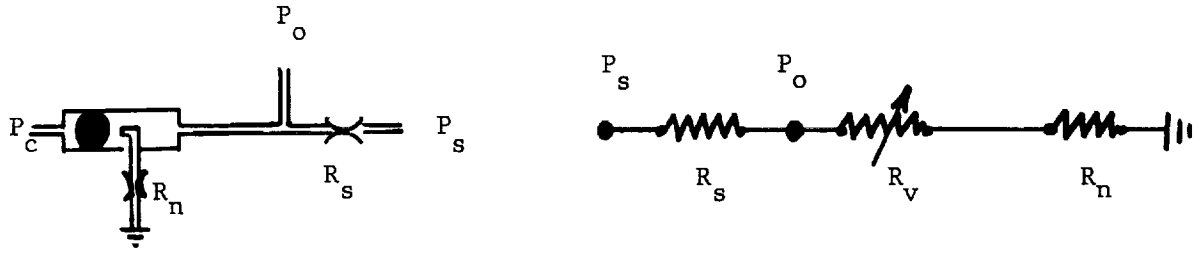

(a) Buffer Amplifier(1:1)

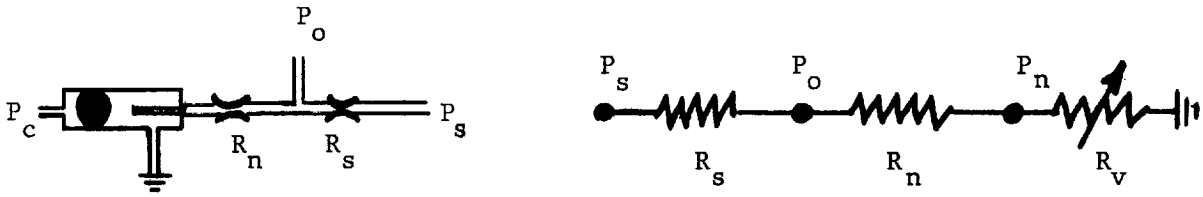

(b) Gain Amplifier

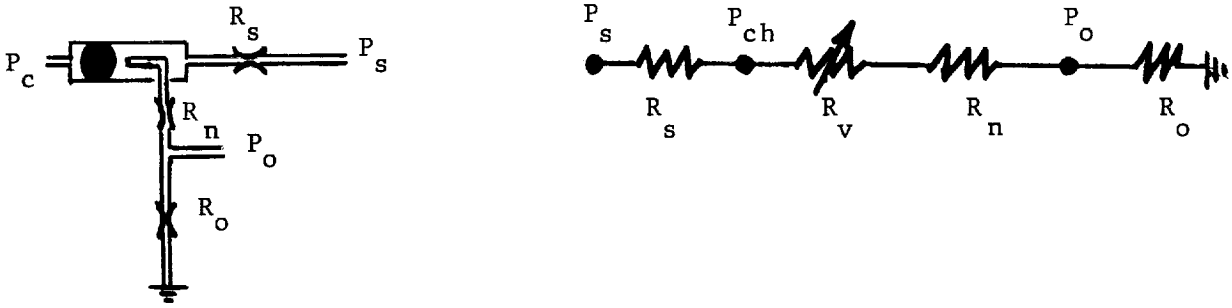

(c) Buffer-gain Amplifier

FIGURE 1 Amplifier Configurations and Equivalent Static Circuits

The gain equation can be obtained directly from the force balance on the bead:

$$p_c A = \pm F_f + p_o A \tag{5}$$

$$G = \frac{\partial p_o}{\partial p_c} = 1 \mp \frac{1}{A} \frac{\partial F_f}{\partial p_c} \tag{6}$$

Introducing the reasonable assumption that the friction force is independent of the control pressure, the gain is:

$$G = 1 \tag{7}$$

Gain amplifier.--The gain amplifier circuit equations are obtained in reference to Figure 1(b):

$$\frac{p_s}{R_s + R_n + R_v} = \frac{p_o}{R_n + R_v} = \frac{p_n}{R_v} \tag{8}$$

Solving the second equality for the output pressure gives

$$p_o = p_n \left\{ 1 + \frac{R_n}{R_v} \right\} \tag{9}$$

Rearranging the first and the third expressions in equation (8), we have

$$R_v = \left\{ \frac{p_n}{p_s - p_n} \right\} (R_s + R_n) \tag{10}$$

Substituting equation (10) into equation (9) and solving for p_n:

$$p_n = p_o \left\{ 1 + \frac{R_n}{R_s} \right\} - p_s \frac{R_n}{R_s} \tag{11}$$

The bead force balance for the gain amplifier configuration is illustrated in Figure 2. The bead is in equilibrium when:

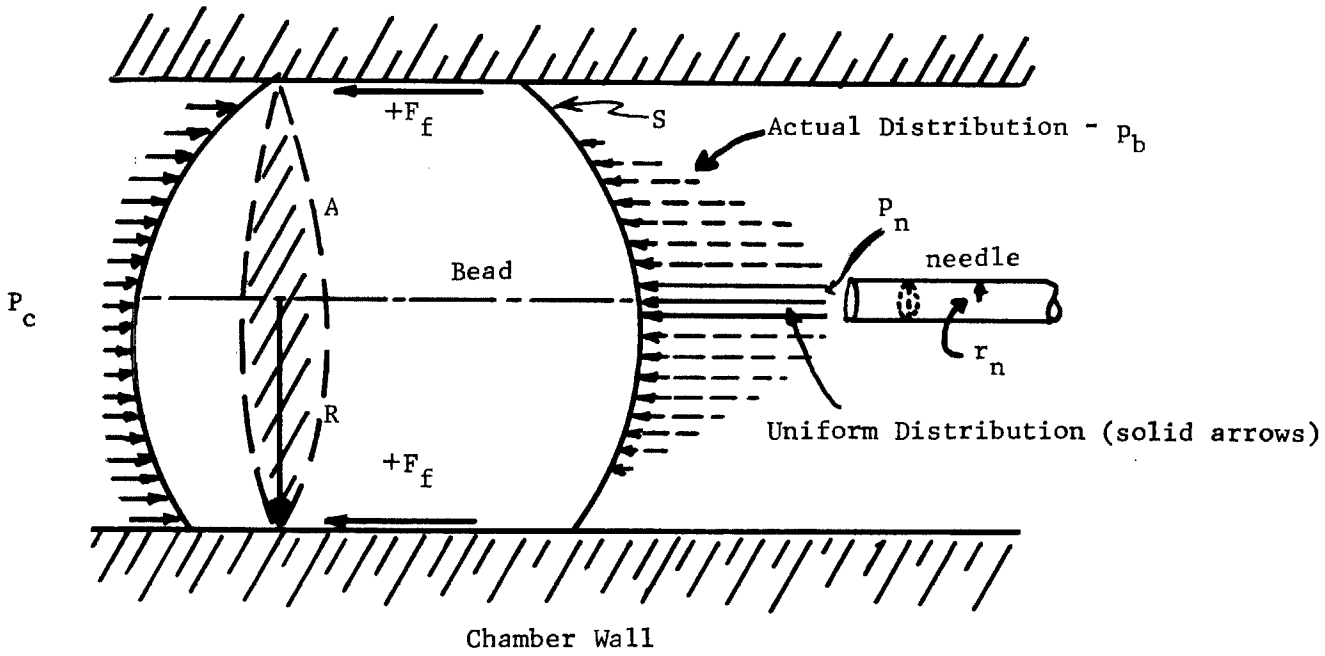

FIGURE 2 Gain Amplifier Force Balance Diagram

$$\int_A p_c dS = \pm F_f + \int_A p_b dS \tag{12}$$

The control pressure on the left-hand side is uniform; therefore, the integral over the cross-sectional area is $p_c A$. The sign of the friction force depends on the direction of the motion.

The integral of the pressure distribution over the bead surface gives the total force exerted on the output side of the bead. This pressure distribution is the total pressure consisting of the sum of the dynamic pressure and the static pressure. The dynamic pressure is a function of the jet velocity while the static pressure depends mainly on the proximity of the bead. Therefore:

$$p_b = p_{st} + p_d \tag{13}$$

As a first approximation, it will be assumed that the dynamic pressure is negligible. Thus equation (12) becomes:

$$p_c A = \pm F_f + \int_A p_{st} dS \tag{14}$$

The integral may be written formally:

$$\int_A p_{st} dS = A p_{ave}. \tag{15}$$

where p_{ave} is the average taken over the chamber cross-sectional area. This average can also be written in terms of a fraction k of the maximum center-line pressure p_n:

$$\int_A p_{st} dS = k A p_n \tag{16}$$

Substituting equation (16) into (14) and using p_n to couple the bead-needle system to the circuit equation (11), we obtain:

$$p_c A = \pm F_f + kA\left[p_o\left(1 + \frac{R_n}{R_s}\right) - p_s \frac{R_n}{R_s}\right] \tag{17}$$

Differentiating the output pressure with respect to the control pressure, we have:

$$G = \frac{\partial p_o}{\partial p_c} = \left(1 - \frac{R_n}{R_s + R_n}\right)\frac{1}{k} \tag{18}$$

where

$$k = \frac{1}{Ap_n} \int_A p_{st} dS \ . \tag{19}$$

The quantity inside the brackets is maximized by choosing the values of the needle resistance and the supply resistance in such a way that the ratio of the resistances in the brackets is very small. Then the quantity inside the brackets will approach one, and the gain will approach 1/k. Then, since the pressure distribution on the output side of the bead determines the value of k, the gain of the device is a direct function of that pressure distribution.

For example, for a uniform pressure distribution across the needle diameter (an assumption made in the early stages of this development),

$$k = \frac{2\pi \int_o^{r_n} r p_b dr}{Ap_n} = \frac{a}{A} \tag{20}$$

where $$p_b = \begin{cases} p_n \text{ for } 0 < r \leq r_n \\ 0 \text{ for } r > r_n \ . \end{cases}$$

In this case the maximum gain is then:

$$G = \frac{A}{a} \tag{21}$$

That is, the gain of the device is the ratio of the control chamber area to the needle area.

However, experiments discussed in more detail later in the report have shown that a more realistic pressure distribution may be expressed by:

$$p_b(r) = p_n e^{-r/nr_n} \tag{22}$$

where r_n is the needle radius, and n (to be discussed later) is a factor relating the needle radius to the pressure distribution shape. Then,

$$k = \frac{2\pi \int_o^R re^{-r/nr_n}\, dr}{A} = 2n^2\left(1 - \frac{R}{nr_n} e^{-R/nr_n} - e^{-R/nr_n}\ \frac{a}{A}\right) \tag{23}$$

In the configurations used the ratio R/nr_n is of the order of 10, at least. Therefore, the last two terms inside the bracket are small compared to unity. Then:

$$G = \left(\frac{1}{2n^2}\right)\frac{A}{a} \tag{24}$$

Buffer-gain amplifier.--The buffer-gain amplifier depicted in Figure 1(c) is simply a variation of the buffer amplifier described above. With the introduction of the proper resistances, this amplifier can be operated with a gain larger than unity. In reference to the equivalent circuit shown in Figure 1(c), the circuit equation is:

$$\frac{p_s - p_{ch}}{R_s} = \frac{p_o}{R_o} \tag{25}$$

Solving for the chamber pressure:

$$p_{ch} = p_s - p_o \frac{R_s}{R_o} \tag{26}$$

The bead force-balance equation is:

$$p_c A = \pm F_f + p_{ch} A \tag{27}$$

Substituting (26) into (27), we have

$$p_o = \left(p_s - p_c \pm \frac{F_f}{A} \right) \frac{R_o}{R_s} \tag{28}$$

Taking the partial derivative of the output pressure with respect to the control pressure, we obtain the gain:

$$G = \frac{\partial p_o}{\partial p_c} = - \frac{R_o}{R_s} \tag{29}$$

That is, the gain is equal to the ratio of the output resistance to the supply resistance. Therefore, by connecting the original unity-gain buffer amplifier into the circuit shown in Figure 1(c), it is possible to achieve a high gain which, like an operational amplifier, is only dependent on two fixed, passive restrictors.

Dynamic Analysis

Buffer Amplifier -- The study of the dynamic behavior of the buffer amplifier must take into account the response of the input and output circuits and the dynamics of the bead itself. The main characteristics of the input and output circuits are determined by the presence of resistances and of the chamber capacitances formed on each side of the bead. These are shown in Figure 3(a). The bead dynamics are those of a spring-mass system with damping. The effective spring is provided by the compression of the air at both sides of the bead. Also, in order to preserve a simple analytical model, the friction phenomena are linearized into an effective viscous damping coefficient. A schematic of the bead dynamic system is shown in Figure 3(b) and the equivalent spring-mass system is shown in Figure 3(c).

A block diagram of the buffer amplifier dynamic system is shown in Figure 4(a). In order to obtain the various transfer functions, we will consider each of the components of the circuit in some detail.

Input circuit - With reference to Figure 3(a) we see that the input circuit consists of a simple RC-series circuit with the transfer function

$$\frac{P_c'}{P_c} = \frac{1}{1 + T_i s} \tag{30}$$

where $T_i = R_c C_c$, and s = Laplace transform variable.

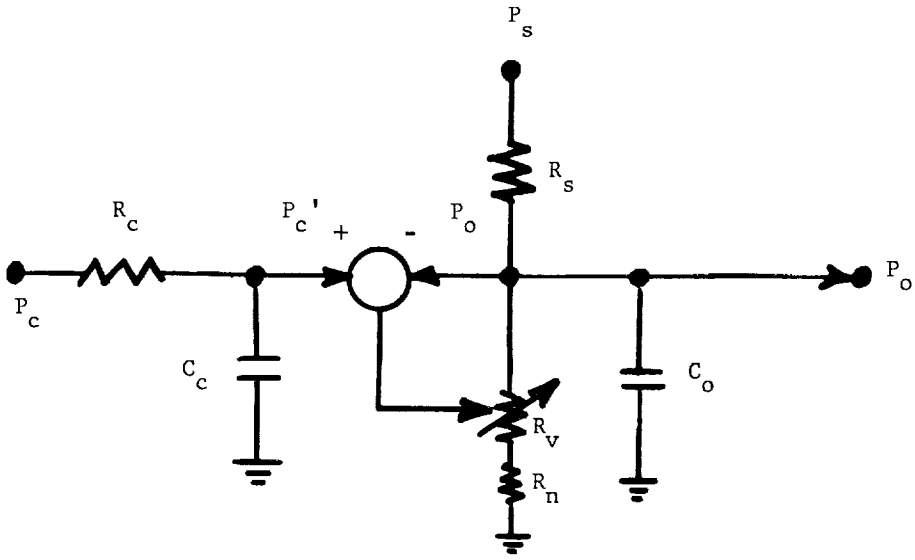

(a) Dynamic Equivalent Circuit

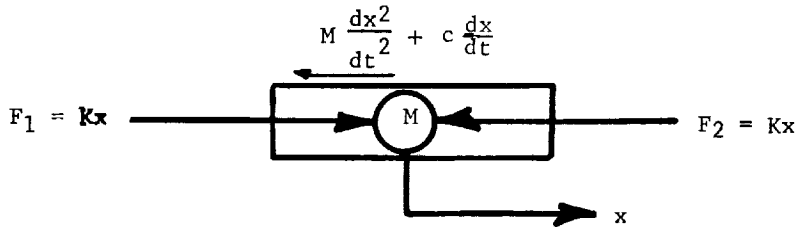

(b) Dynamic Force Balance

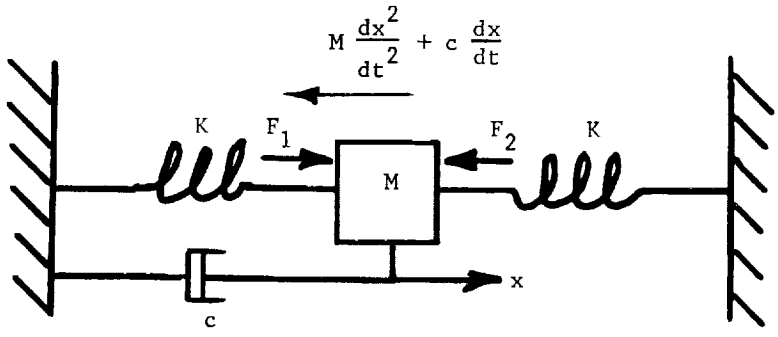

(c) Spring-Mass Analog

FIGURE 3 Equivalent Dynamic Circuits

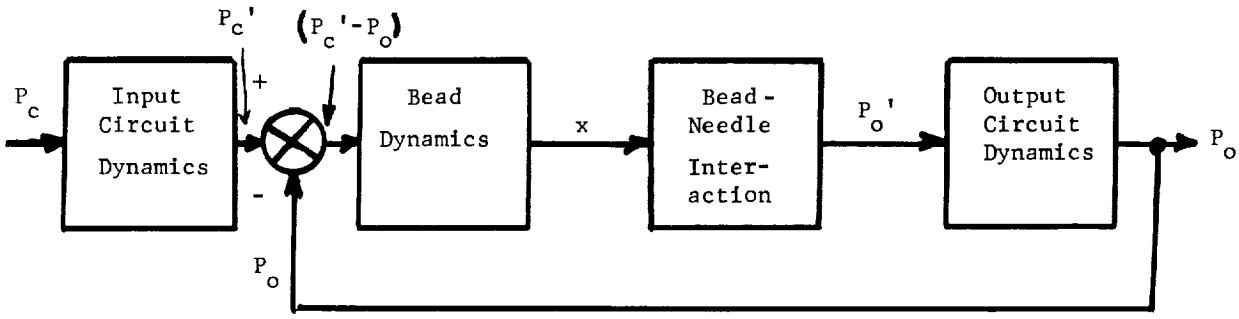

(a) Block Diagram of Buffer Amplifier System

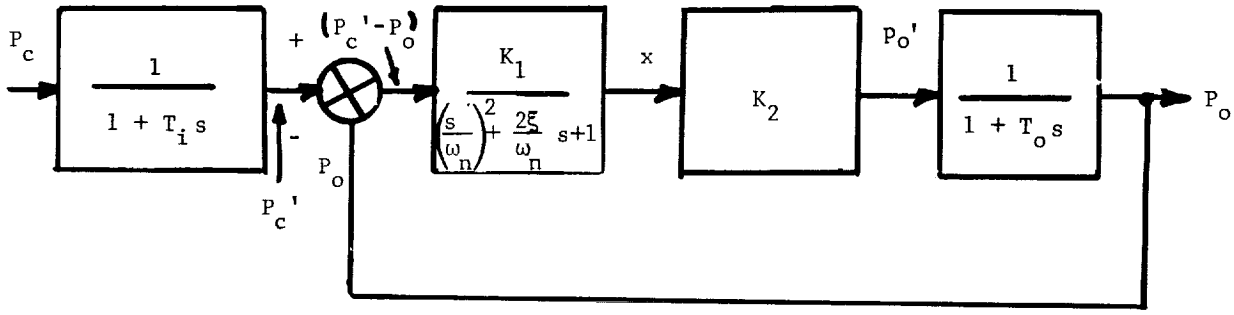

(b) Block Diagram of Buffer Amplifier System
With Transfer Functions

FIGURE 4 Block Diagrams

Output circuit - The output circuit similarly has the following transfer function:

$$\frac{P_o}{P_o'} = \frac{1}{1 + T_o s} \tag{31}$$

where $$T_o = \frac{R_s(R_v + R_n)}{R_s + R_v + R_n} C_o$$

Bead-needle interaction - The bead-needle interaction will be considered as a pure gain. Therefore, its transfer function is:

$$\frac{P_o'}{X} = K_2 \tag{32}$$

Bead dynamics - In reference to Figure 3(b) we have, by the balance of forces on the bead:

$$M \frac{d^2x}{dt^2} + c \frac{dx}{dt} + 2Kx = 0 \tag{33}$$

The spring forces in the ends of the chamber result from the compression of the trapped fluid. Assuming adiabatic compression we find that the effective spring constant K for small deviations of the bead from its equilibrium position is:

$$K = \frac{\partial F}{\partial x} = \frac{\gamma p A}{x_o} \tag{34}$$

where γ = ratio of specific heats.

Substituting into the force equation we have

$$M \frac{d^2x}{dt^2} + c \frac{dx}{dt} + \frac{2\gamma p A}{x_o} x = 0 \tag{35}$$

The transfer function of the bead is

$$\frac{X}{P_c' - P_o} = \frac{K_1}{\frac{s^2}{\omega_n^2} + \frac{2\xi}{\omega_n} s + 1} \tag{36}$$

where K_1 = gain factor

$$\xi = \frac{1}{2} \frac{C}{\sqrt{2MK}} = \text{Damping factor} \tag{37}$$

and the undamped natural frequency of vibration is

$$\omega_n = \sqrt{\frac{2K}{M}} \tag{38}$$

These transfer functions have been introduced in the block diagram in Figure 4(b). Thus the system has a forward-loop transfer function.

$$\frac{P_o}{P_c' - P_o} = \frac{K_1 K_2}{(1 + T_o s)\left[\left(\frac{s}{\omega_n}\right)^2 + \frac{2\xi}{\omega_n} s + 1\right]} \tag{39}$$

where K_1, K_2 = gain factors

P_o = output pressure

P_c' = control pressure

The system has an overall closed-loop transfer function:

$$\frac{P_o}{P_c} = \frac{1}{(1 + T_i s)\left[1 + \frac{(1 + T_o s)}{K_1 K_2}\left\{\left(\frac{s}{\omega_n}\right)^2 + \frac{2\xi}{\omega_n} s + 1\right\}\right]} \tag{40}$$

where T_i = time constant - input circuit.

From the transfer function (2) it can be seen that for K_1K_2 relatively large, the bead dynamics as well as the output circuit dynamics can be neglected, and the amplifier would then behave essentially as a first-order system. Its dynamic characteristic would then be determined by the time constant of the control circuit, i.e.

$$\frac{P_o}{P_c} = \frac{1}{1 + T_i s} \tag{41}$$

Gain Amplifier -- The gain amplifier dynamics are the same as those of the buffer amplifier, except that a gain factor will appear in the numerator of the transfer function:

$$\frac{P_o}{P_c} = \frac{G}{(1 + T_i s)\left\{1 + \frac{(1 + T_o s)\left[\left\{\frac{s}{\omega_n}\right\}^2 + \frac{2\xi}{\omega_n} s + 1\right]}{K_1K_2}\right\}} \tag{42}$$

where

$$G = \left\{1 - \frac{R_n}{R_s + R_n}\right\} \frac{1}{k} \quad \text{(equation 18).}$$

(See the static analysis of the gain amplifier above.)

Buffer-Gain Amplifier -- The buffer-gain amplifier will have a transfer function of the same form as (42); that is,

$$\frac{P_o}{P_c} = \frac{-R_o/R_s}{(1 + T_i s)\left\{1 + \frac{(1 + T_o s)\left[\left\{\frac{s}{\omega_n}\right\}^2 + \frac{2\xi}{\omega_n} s + 1\right]}{K_1K_2}\right\}} \tag{43}$$

Stability Considerations

In the previous section it was shown that, by using high open-loop gain, the amplifier can be made to behave dynamically as a first-order system. The question then arises as to the range of gain values in which the amplifier remains stable. This question is best answered

by computing the stability boundary for various values of the circuit parameters such as the open-loop gain, output circuit time constant, bead natural frequency, and damping factor. To simplify the problem a damping ratio, ξ, of .7 has been chosen and the stability boundary has been plotted for the open loop gain $K_1 K_2$ versus the nondimensional ratio $1/T_o \omega_n$. This is shown in Figure (5). This figure clearly illustrates that stable operation is compatible with high values of the open-loop gain and that the representation (41) is valid. For example, for values of $1/T_o \omega_n$ larger than 17 and smaller than .05 the open-loop gain $K_1 K_2$ can be as large as 25 and the system will be stable.

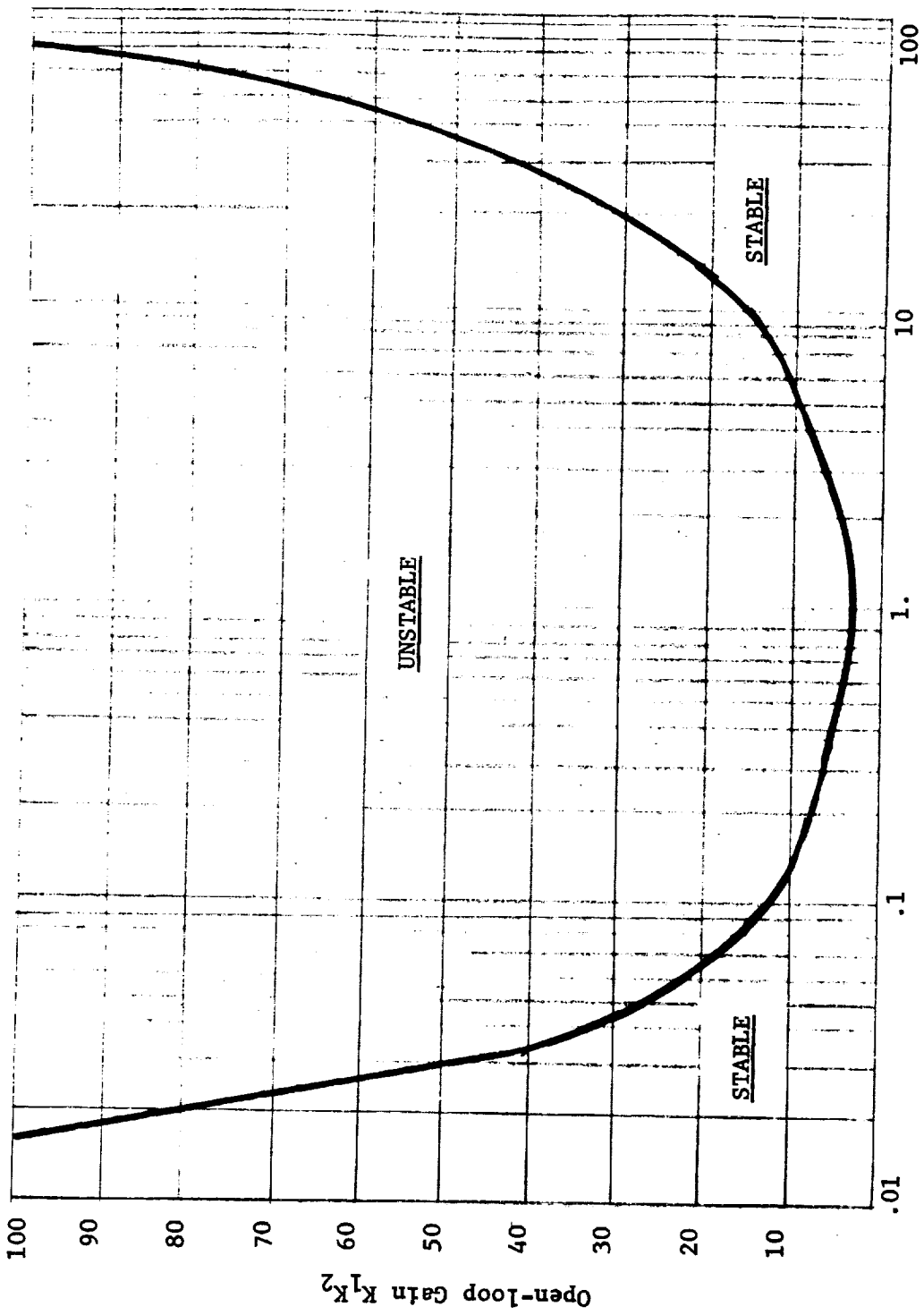

FIGURE 5 - Stability Boundary for Open-loop Gain Versus Output Circuit Time Constant and Bead Natural Frequency

CHEMICAL STUDIES*

A preliminary chemical investigation was carried out to determine what non-toxic liquids or combination of liquids and solid coatings would exhibit properties similar to those of mercury.

Several liquids were enclosed in a buffer amplifier and investigated for air bleed action. The amplifier consisted of a liquid bead whose surface functioned as a diaphragm against a stainless steel capillary tube, a chamber of 1/3" I.D. Plexiglas (polymethylmethacrylate) tubing, and air inlet aluminum plugs in each end.

All inner surfaces of the amplifier were treated with Zepel (water and stain repeller from DuPont) by spray application. The stainless steel capillary had its interior treated by the use of a medical stainless steel needle syringe which allowed copious amounts of the Zepel solution to bathe the inner chamber and the stainless steel capillary bleeder. All parts were heat cured at 60^{o} C for 15 minutes. (Extreme care was taken to avoid dust in the chamber.)

The Zepel surface coating is the all-important single ingredient with respect to air bleeder action. Zepel surface-coating produces two very useful effects:

1. since most liquids will not wet the surface coated with Zepel, a convex liquid surface is produced;
2. Zepel treatment of a capillary tube reverses the capillarity effect.

The effect on capillarity of the Zepel-treated surface was used as a guide for the selection of liquids to be used as bead materials in the amplifier. Obviously, those liquids which demonstrate a high reversal of capillarity are preferred for these reasons: (a) the liquid surface will behave as an ideal diaphragm at the entrance of a fine-bore tube (such as a stainless steel bleeder tube) and (b) the liquid will not be forced out the capillary tubing.

A wide range of polar to nonpolar liquids and mixtures of liquids were evaluated using the reversal-of-capillarity technique. The following liquids were outstanding:

1. water
2. glycerine
3. water + glycerine mixtures (20-70% glycerine by weight)
4. glycerine + water + $FeCl_3$.

*This work was carried out by Dr. L. L. Pytlewski of the Drexel Institute of Technology.

In addition to the reversal of capillarity at the bleeder tube the liquid bead is required to remain in place so that only the surfaces deform. Although the Zepel surface coating prevents "wetting" of liquids at the surface, there is a "spreading" factor which comes into play and for the liquids—water, glycerine, water + glycerine, and water + glycerine + $FeCl_3$—all "spread" well enough not to be moved about in the Plexiglas chamber until air pressures much greater than those required for operation (some sizable fraction of the initial air supply set at 5 $lb/in.^2$) of the amplifier were applied.

Of course, if the Plexiglas chamber is not treated with Zepel, then wetting of Plexiglas will occur and the resistance to movement is substantially increased. However, the convexity of the bead surface will be reduced (or removed) and thus the diaphragmic character of the liquid surface is changed.

Because of their greater surface-tension-to-density ratio, these liquids are not significantly affected by the gravitational sag that takes place with mercury. Thus, airtight seals of bead and container surface are produced, and the beads are less affected by acceleration.

In total, a collection of some forty new single organic liquids were tested in the experimental amplifier. As a result it has been concluded that the glycerine-water systems listed above are optimum for the application. In effect, glycerine, water, and glycerine-water mixtures have demonstrated most of the desired qualities required by a liquid bead in the analog buffer amplifier.

It has been found that proper bleeder action is attained using any one of the glycerine-water liquid systems, whether the container tubing is treated with Zepel or not, as long as the stainless steel bleeder tube is coated with Zepel.

Additionally, it was found that a common paraffin wax coating on the surfaces of the analog amplifier produced effective responses using glycerine-water mixtures. As long as water is present, the paraffin wax coating is effective.

Tests were also run using a silicone coating (polymethoxysilane) and glycerine and water mixtures, and the silicone was found to be ineffective.

In summary, three different basic chemical system configurations were tested:

1. a Zepel-coated Plexiglas or glass tube, 1/8" I.D. or less, employing a liquid diaphragm;
2. a liquid bead coated with "Organosil - S-5", in the same chamber as above; and
3. water or glycerine drop in a chamber with silicon-oil-coated walls.

Using glycerine in the liquid phase indicates that System #2 appears to show the greatest potential because it exhibits the most favorable physical characteristics and because there is no "bubble through" at the vicinity of the small inlet pressure duct.

EXPERIMENTS

Experimental Setup

Static tests.--A number of amplifier units (see Figures 6(a) and 6(b) for illustration of typical units) were tested statically in the circuit shown in Figures 7 and 8. The control pressure was applied by a manually controlled bleed arrangement. The supply pressure consisted of a regulated constant-pressure source. The resistors used were Conrac-developed linear components; they consisted of bundles of 10-mil capillary tubes connected in parallel. All pressures were measured in vertical manometers.

Dynamic tests.--For the dynamic tests, a sinusoidally varying control pressure was provided by a 30-watt acoustic driver energized by an audio-frequency signal generator through a power amplifier. (See Figure 9 and 10 for the experimental dynamic test arrangement.) The acoustic driver generated a control pressure that oscillated from above ambient to below ambient. In the below ambient part of the cycle, the bead tended to be drawn out of the chamber. To avoid this, a slight bias pressure was superimposed on the control signal, thus keeping the bead operating close to the needle at all times. The input and the output pressure on the amplifier were measured by means of low-volume unbonded strain gauge pressure transducers. The outputs of the pressure transducers were applied directly to a dual-beam oscilloscope. The traces on the oscilloscope were photographed for each frequency point and the data was later reduced from these photographs.

Buffer Amplifier Test Results

Static curves.--Numerous amplifier configurations were tested at various stages of the development in order to obtain information as to the effect of chamber size, supply pressure, needle diameter, and other parameters on the static characteristics of the device.

Figure11 shows typical results with two buffer amplifier units having two different chamber diameters, and tested at two different supply pressures. As expected, the amplifier curves show a linear range with monotonic curves approaching asymptotes for the lower and upper ranges of control pressures. At the upper limit (for the smaller diameter units) we have the saturation level corresponding to the complete shut-off of needle (or bleeder) flow, with the output pressure climbing up to the value of the supply pressure (see equation (4)). At the lower end, the output pressure corresponding to zero control pressure is determined by the values of supply and fixed needle resistance as expressed by equation (3) of the mathematical analysis. The intermediate portion of these curves shows good linearity.

Saturation appears earlier in the larger diameter units. This is due to the premature contact of the bead against the needle tip. Premature contact is most likely to occur in the larger diameter units because of asymmetric gravity deformation (sag) of the bead. This is discussed at

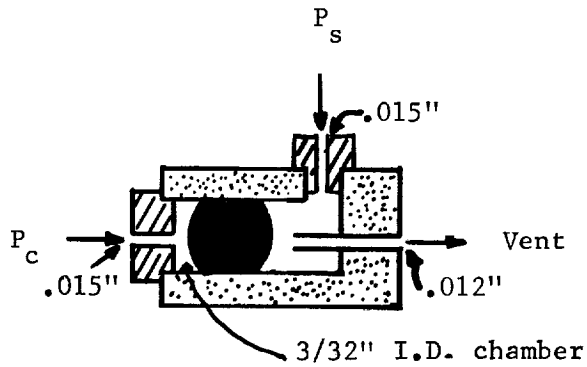

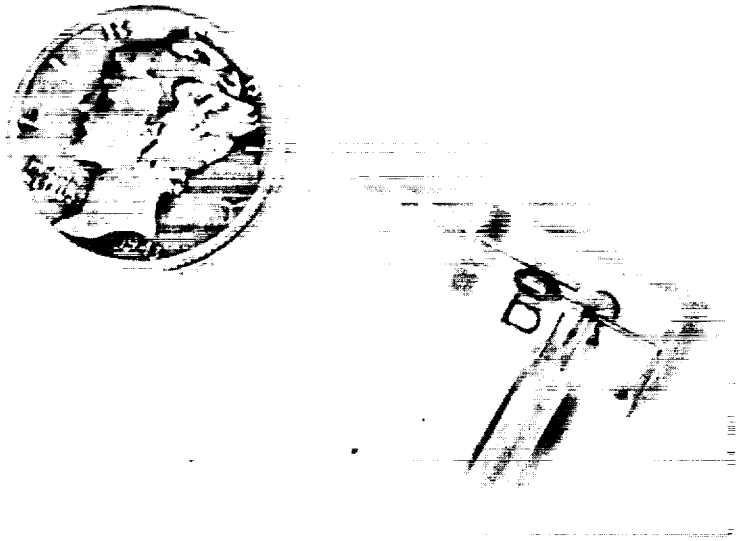

FIGURE 6(a) Buffer Amplifier Configuration

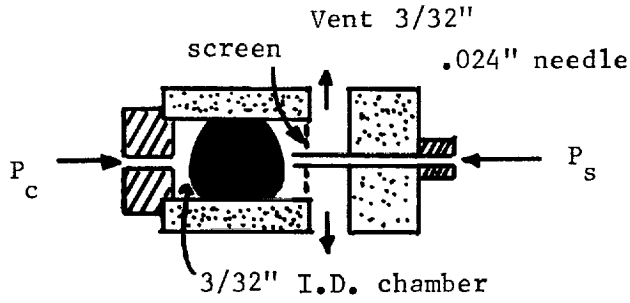

FIGURE 6(b) Gain Amplifier Configuration

FIGURE 7 Static Test Setup

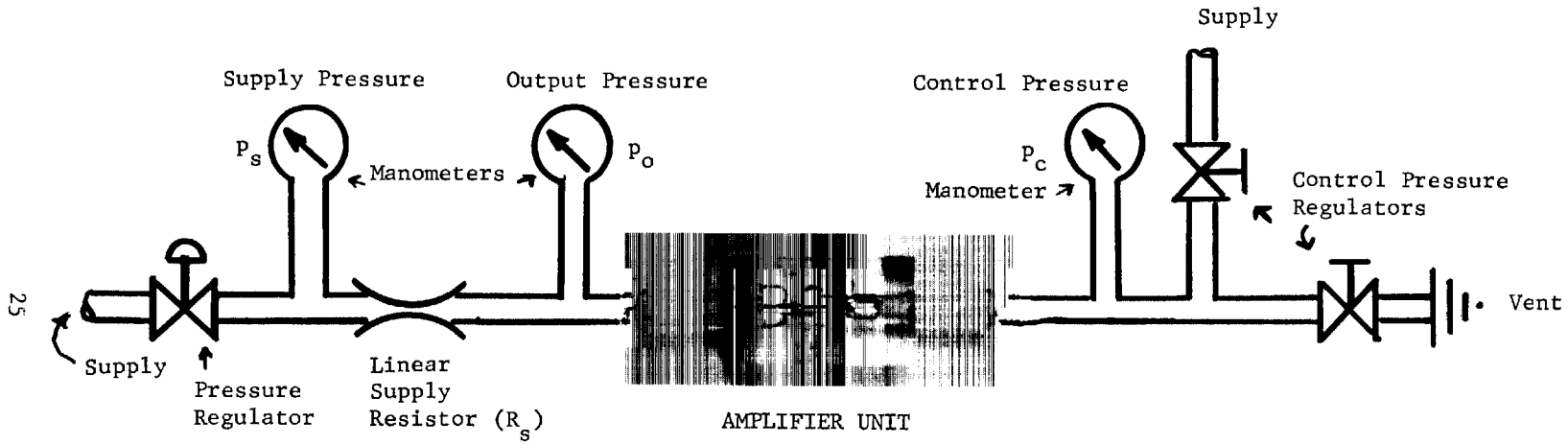

FIGURE 8 Schematic of Static Test Setup

FIGURE 9 Dynamic Test Setup

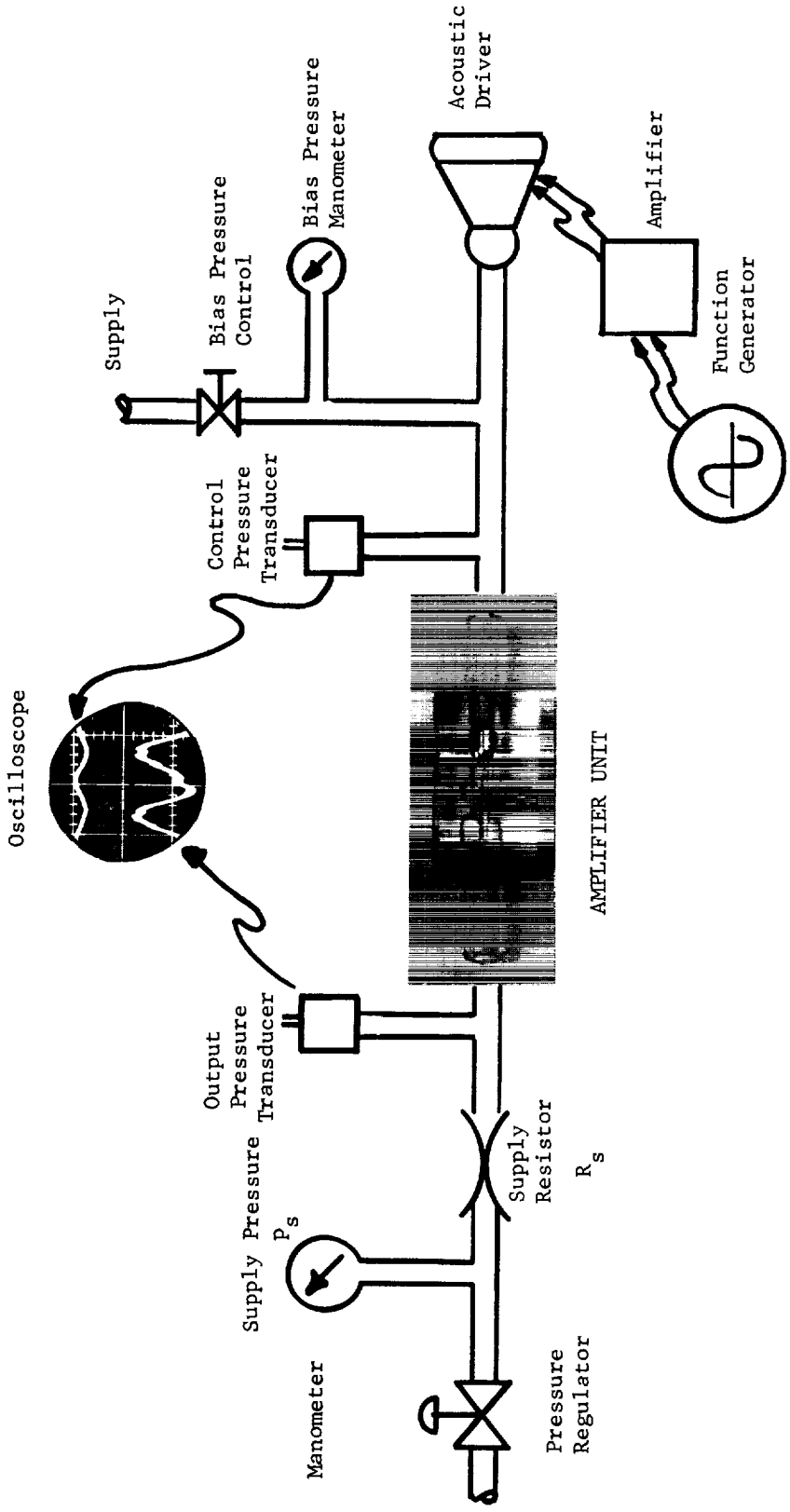

FIGURE 10 Schematic of Dynamic Test Setup

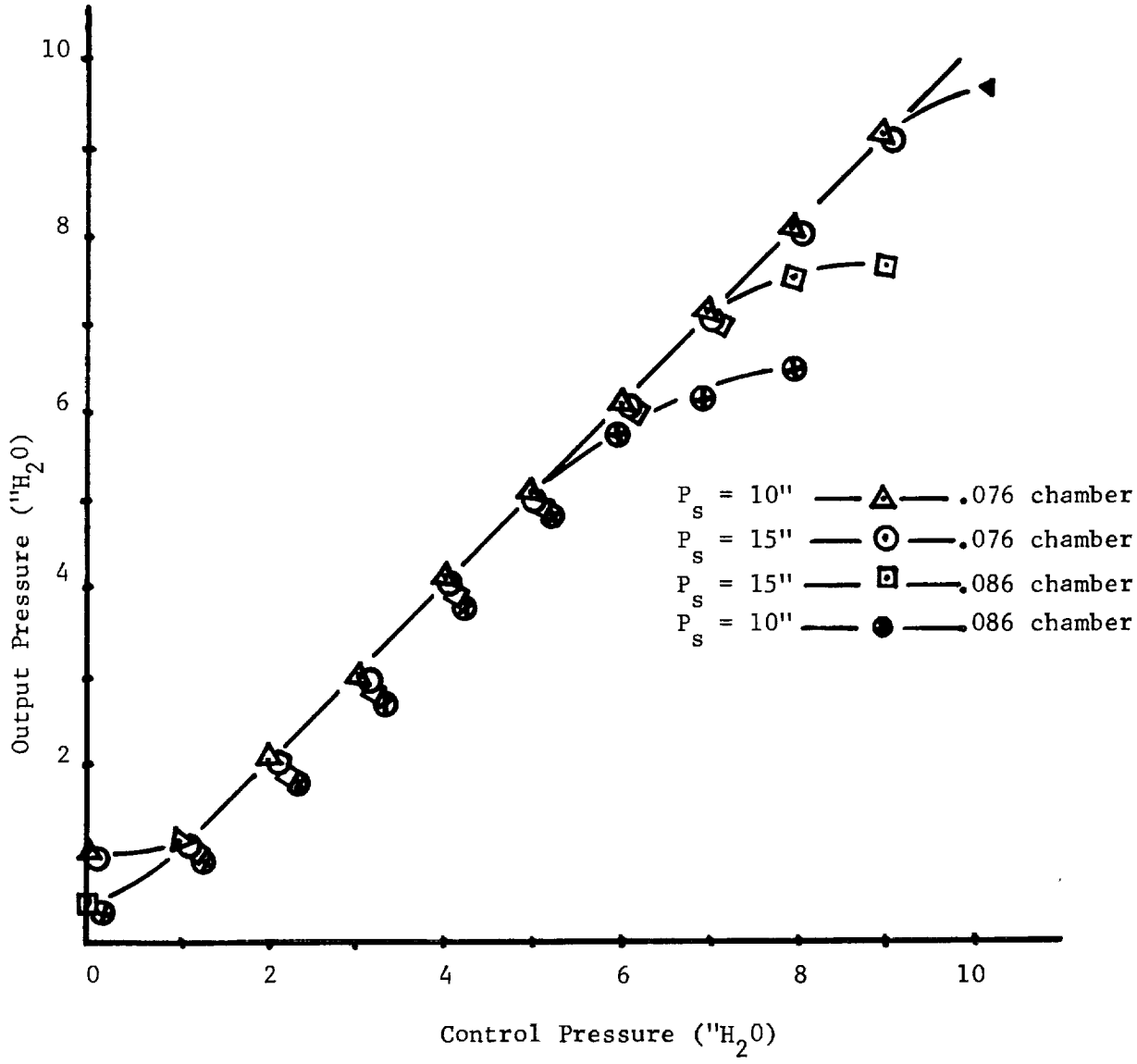

FIGURE 11 Test Buffer Amplifier Static Characteristics

greater length in the next section, Amplifier Development. Figure 12 shows the input-output characteristics of a final prototype buffer amplifier unit.

Dynamic curves--Figure 13 shows the results of tests on two buffer amplifier units having different chamber and bleed needle sizes. These two units exhibit a somewhat non-linear behavior, which is partially due to the uncertainties introduced during the data reduction of the photographs. Nevertheless, it can be seen that their dynamic behavior is that of a system of higher than first, or even second, order. This may be appreciated by the fact that the phase angle appears to be increasing beyond 180^{o} (lag). It seems reasonable to conclude that the condition for eliminating the bead and output circuit dynamics, as stated in the dynamic analysis, has not been fulfilled in these units.

The second-order natural frequencies appear to fall at approximately 25 and 50 hertz. The difference between these two values may be traced to the difference in size (length) of the beads and to some degree, to a smaller bleed needle fixed resistance.

These curves also show that there is a fairly high degree of damping of the bead motion.

Gain Amplifier Test Results

Static curves.--Figure 14 shows the test results of two different gain amplifier units. These two units show the same overall characteristics as the buffer units. The gain is somewhat different on the two units but is approximately 2.5. The gain amplifier units in general display much less linearity than the buffer units. This appears to be due to hysteresis in the bead motion, and will be discussed in more detail in the developmental section. Figure 15 shows the input-output characteristics of a final prototype gain amplifier unit.

Dynamic tests.--Figure 16 shows the frequency response of four different units. As did the buffer units, the gain units in general show an apparent non-linear characteristic. Their natural frequencies range from about 20 to 40 hertz and their second-order response shows effective damping factors ranging from .5 to .9. Units (C) and (D) show a phase lag that appears to approach 180^{o} asymptotically. Therefore they may be considered essentially second-order systems. Units (A) and (E), however, exhibit lag angles increasing beyond 180^{o}.

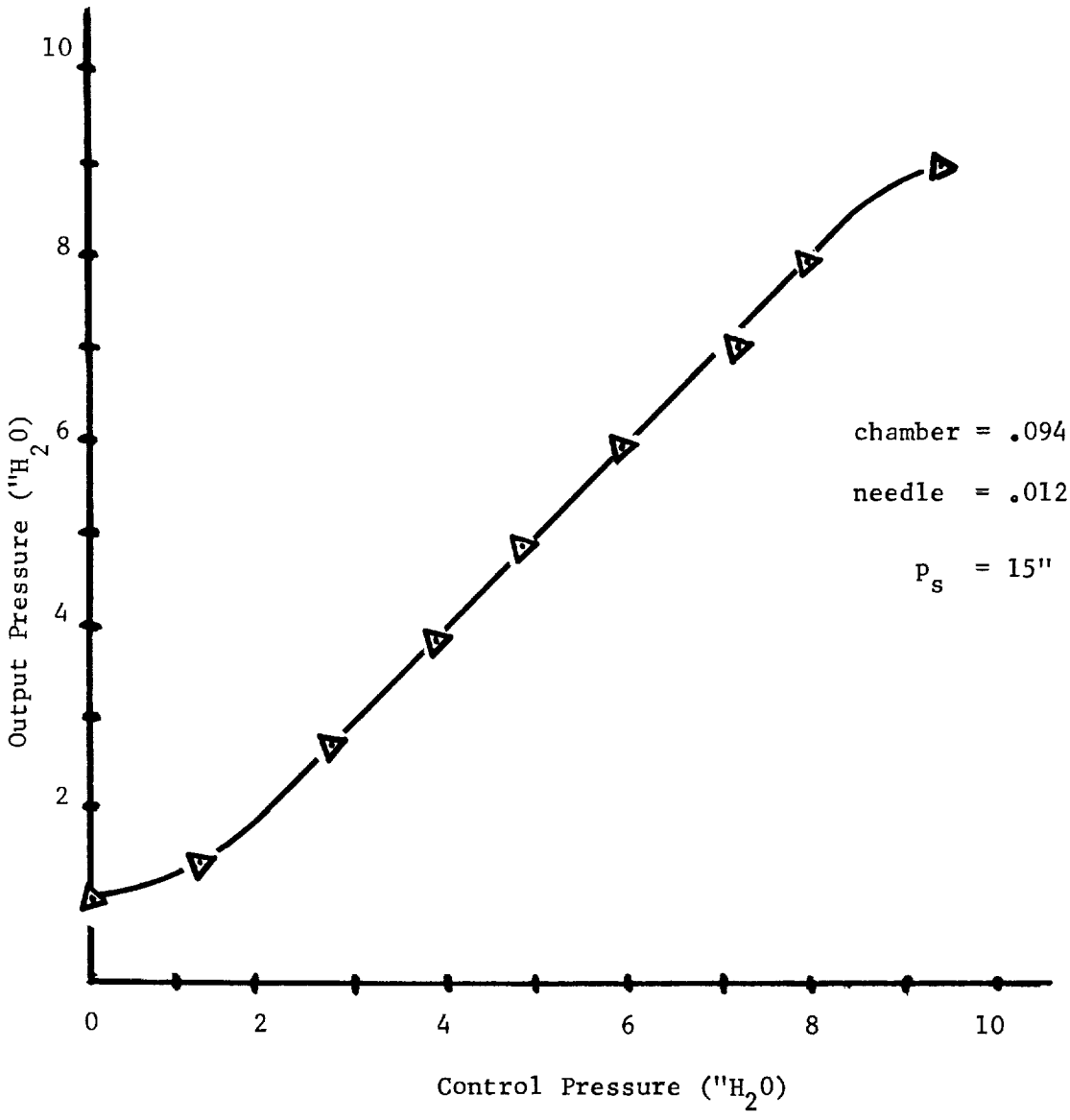

FIGURE 12 Final Buffer Amplifier Static Characteristics

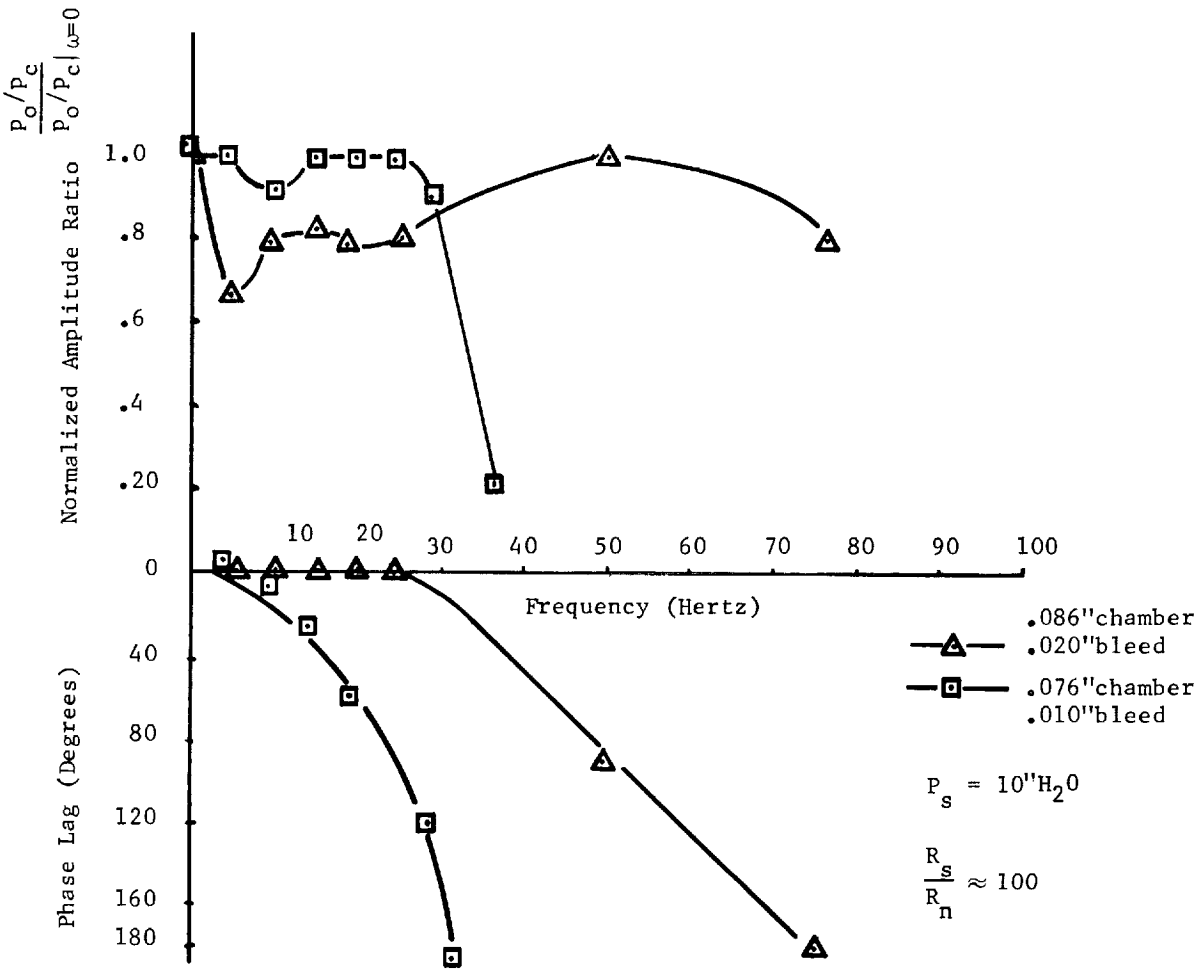

FIGURE 13 Test Buffer Amplifier Dynamic Characteristics

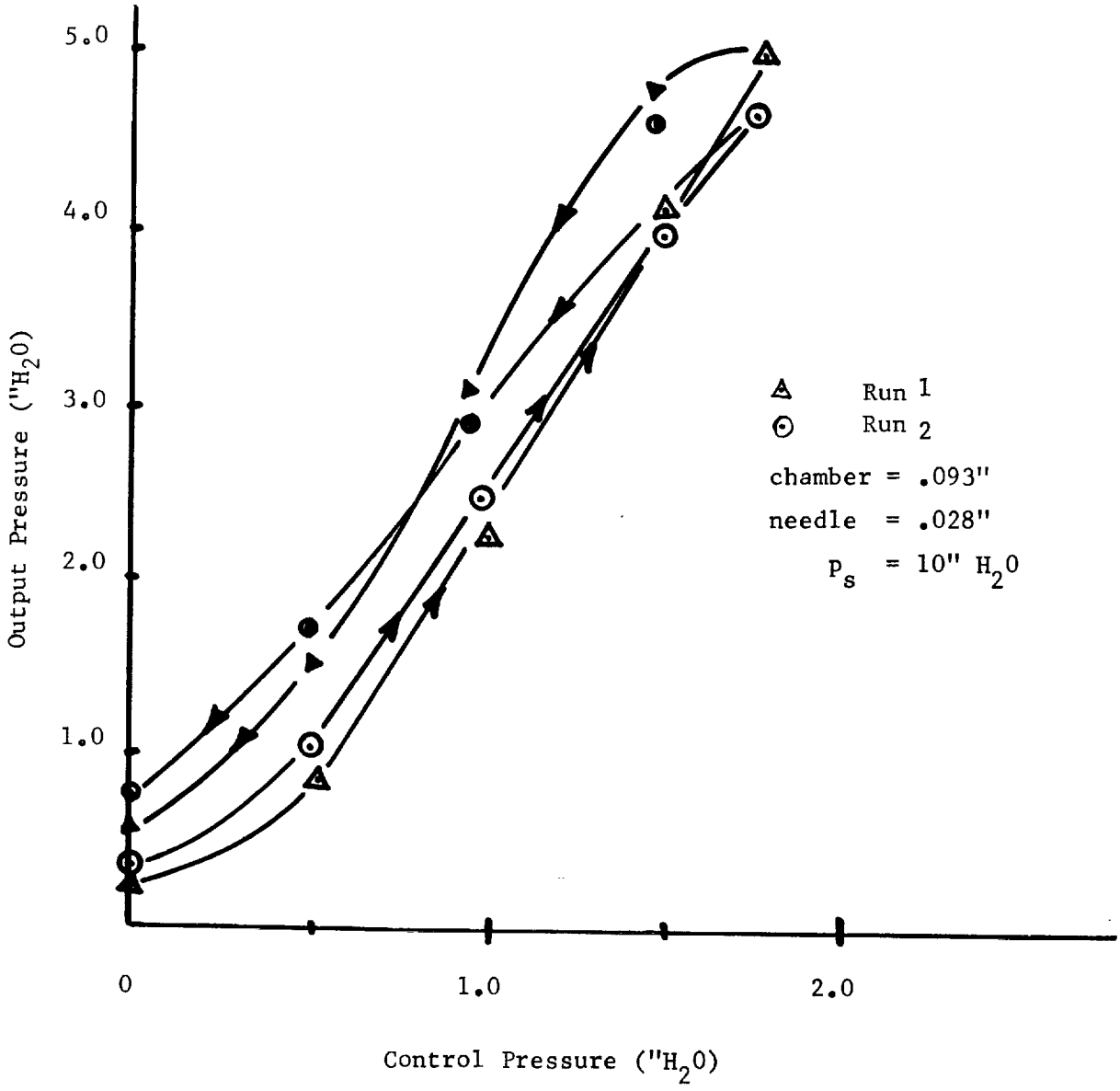

FIGURE 14 Test Gain Amplifier Static Characteristics

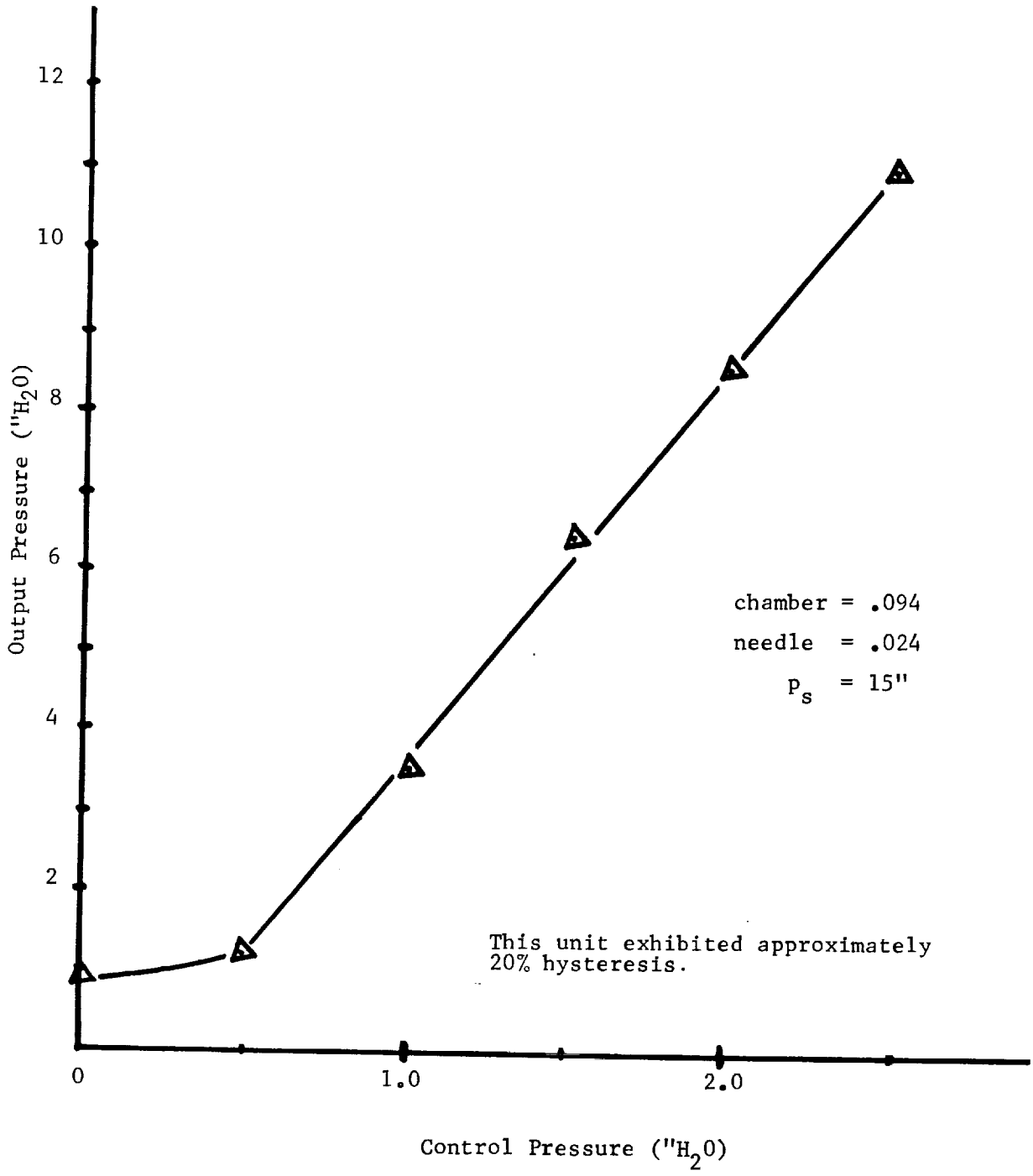

FIGURE 15 Final Gain Amplifier Static Characteristics

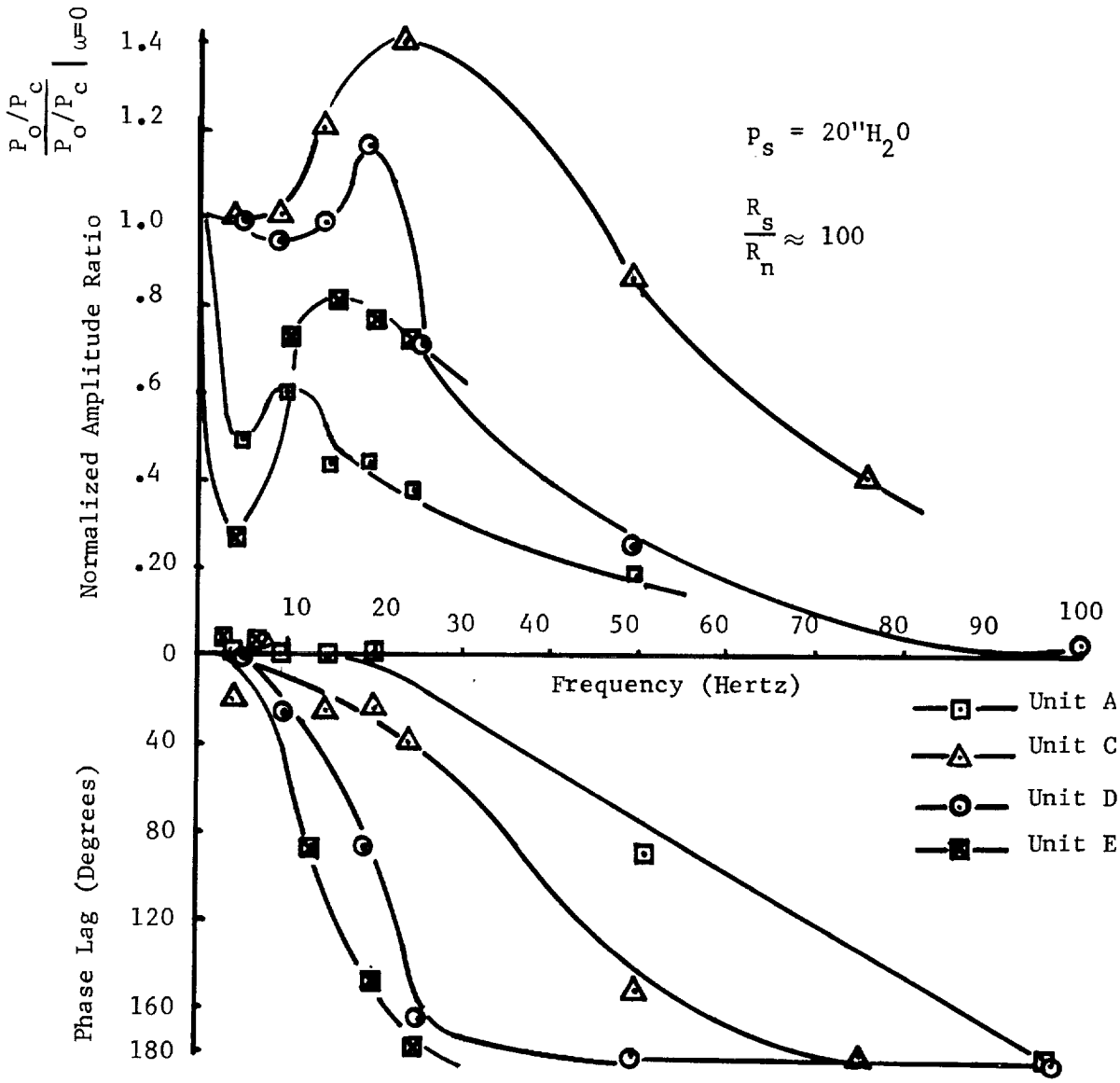

FIGURE 16 Test Gain Amplifier Dynamic Characteristics

Buffer-Gain Amplifier

Figure 17 shows the characteristic curve for a buffer-type unit connected as a gain amplifier (circuit of Figure 1c). The output remains constant as the control pressure increases, until the input and the output are balanced. Then, further increases in the control pressures reduce the output pressure. These units show good linearity. The gain is negative, but considerably higher than in the gain amplifier (above) operating on a difference in areas.

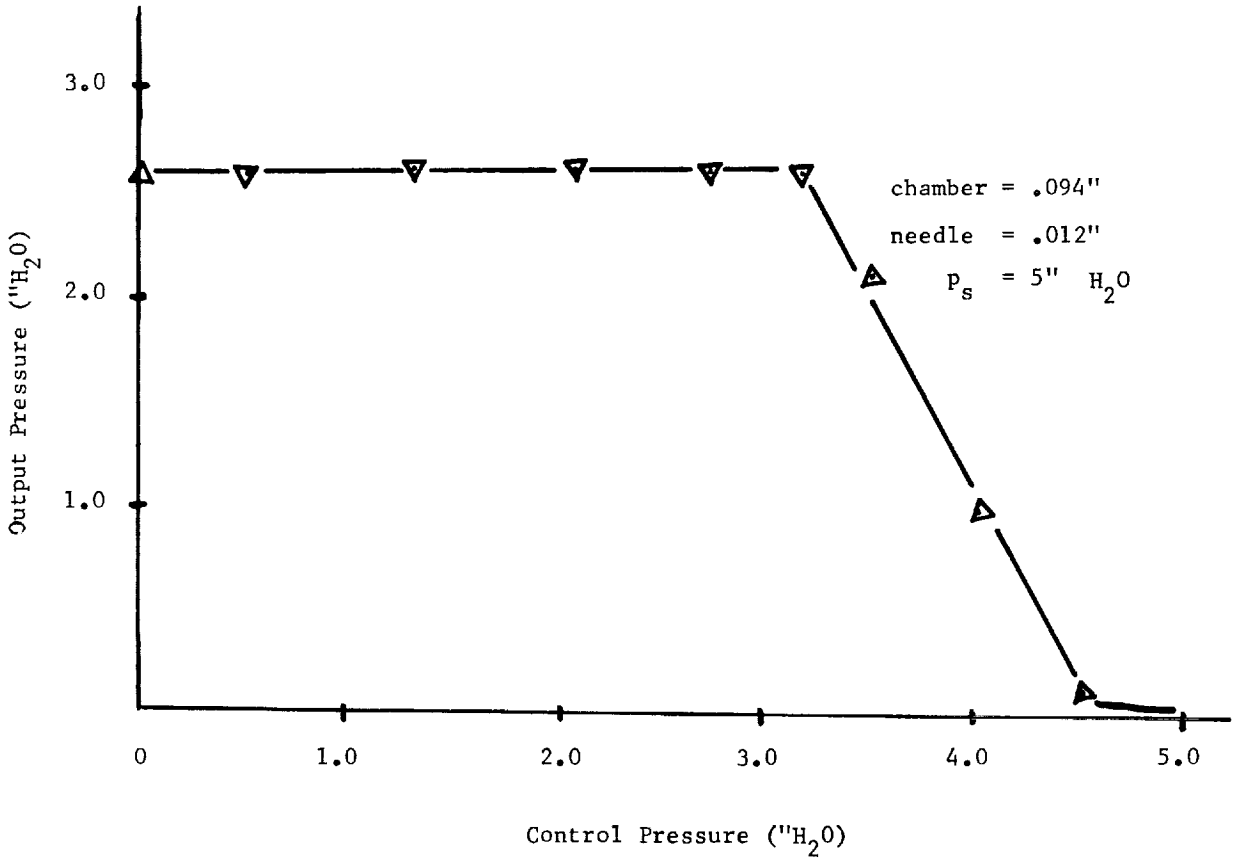

FIGURE 17 Static Characteristics of Buffer-gain Amplifier

AMPLIFIER DEVELOPMENT

At the inception of the program, it was anticipated that an infinite-input-impedance, high-gain amplifier might be produced, based on a design using a high ratio of areas. The concept of infinite input impedance has been achieved in practice, but high gains such as predicted by the original mathematical model have not been realized in this design. That model was based on the assumption that the gain of the unit would be the ratio of the control chamber area to the needle area. This ratio could easily be made of the order of 100. When units constructed in this fashion yielded gains averaging only about 5, a closer investigation of the bead behavior and of the bead-needle interaction was carried out.

Two problem areas were investigated: one, the effect on the bead force balance of non-uniform pressure distribution and dynamic pressure effects, and two, hysteresis effects in the bead motion. Work on the first area has resulted in a more refined mathematical model, the results of which are covered in part in the mathematical analysis and in part in this section. The examination of the second area shows that indeed the bead exhibits friction in its motion in the chamber, and this friction appears amplified on the output of the gain amplifier. As a result, the gain of the amplifier is limited by these factors. In spite of this limitation, the goal of an infinite input impedance amplifier with high gain has been achieved with the buffer amplifier connected into a high-gain circuit.

Large-Scale Model

In order to investigate in more detail the forces acting on the bead output side, an approximately 10-to-1 scale model was built (see Figure 18). The chamber consisted of a 2.375" I.D. tube, a "needle" consisting of a .234" I.D. tube, and the bead, which was made out of clay of approximately spherical shape. The bead fitted tightly into the tube so that no leakage could occur between the clay model and the inner walls of the chamber. Eight total-pressure probes were set along a meridian; the first one was in the center line of the unit, the next three were set .1" apart, and the rest were set .2" apart.

In this model, the area ratio between the chamber and the needle was 100-to-1. The distance between the needle and the bead could be measured within .001". The static pressure in the needle was measured by means of a micromanometer capable of reading .001" of water. The output of the total pressure probes was fed to an 8-manometer tube bank. These manometers graphically display the actual pressure distribution on the surface.

It was not practical to produce flows exactly similar to the ones in the actual amplifier. To maintain the same Reynolds numbers as the original flow would have required such low velocities that measurements would have become very difficult, if not impossible. Experiments were run at as low Reynolds numbers as was practical, the actual Reynolds number was about 12,000 while the model Reynolds number was approximately 4,000 and the over-

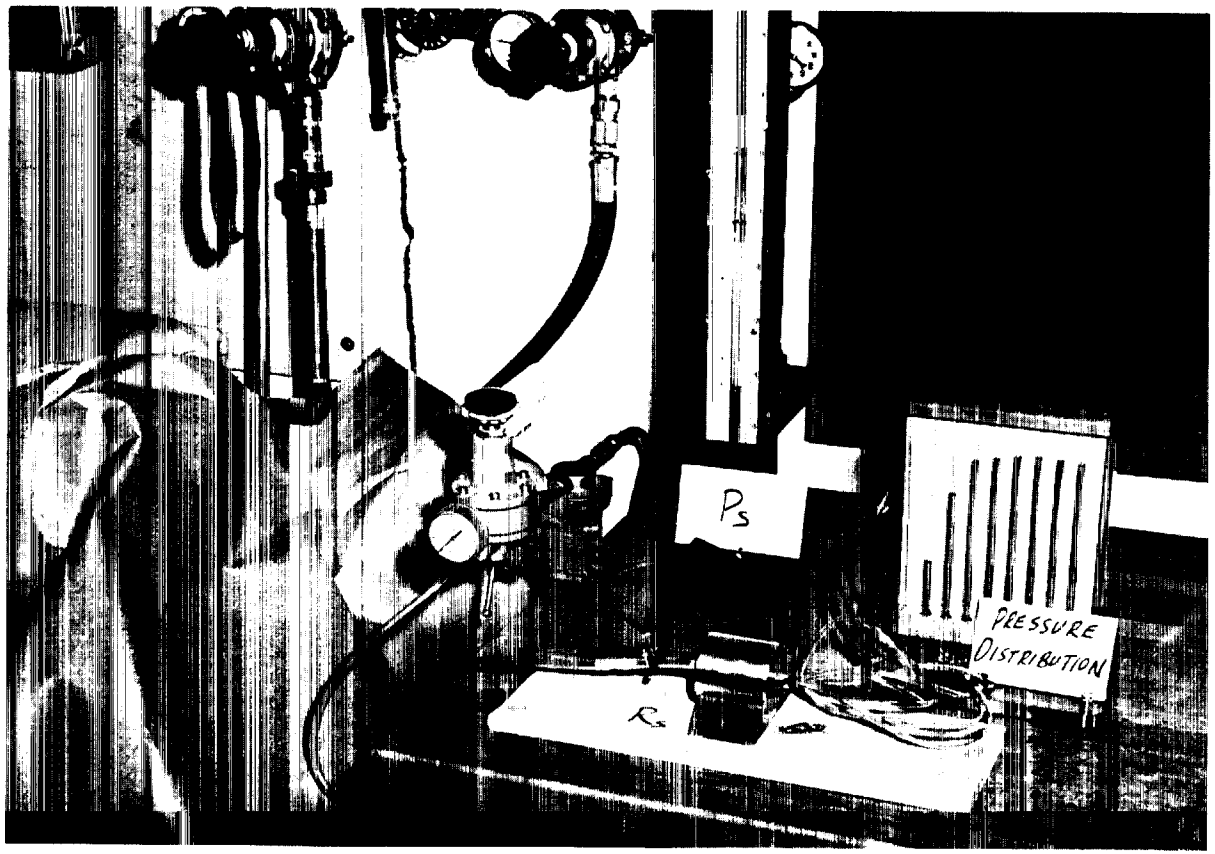

FIGURE 18 Large Scale Model of Gain Amplifier Showing Pressure Distribution Across Bead Surface

all simulation may be considered good.

Pressure distributions obtained from this model are reasonably well described by the distribution shown in equation (22) of the mathematical development. The experimental distributions were used to calculate the value of the parameter nr_n in order to determine the actual curve. This value was found to be about .15" for a needle-bead distance of one needle diameter. From this, we may calculate n which then may be substituted in equation (24) that for an area ratio of 100 to one, predicts a gain of 30 for the gain amplifier. Clearly, the fact that a non-uniform pressure distribution is acting on the output side of the bead is not sufficient to explain the low gain values obtained from the actual amplifier unit (Figure 15).

The remaining discrepancy led to investigations of the effect of the dynamic pressure on the bead force balance. Here, we are distinguishing between the static pressure which reflects on the output circuit by affecting the flow rate, and the dynamic pressure due to the impingement of the needle jet on the bead that causes a force on that bead. This latter pressure however, does not appear in the output.

Therefore, measurements of the static and dynamic pressures were obtained at the surface of the bead for various bead-needle distances. These are shown in Figure 19. It can be seen that the static pressure decays very rapidly as the distance increases between the needle and the bead. As may be expected, the change in the dynamic pressure is imperceptible up to bead-needle distances of the order of one-needle radius. Proper operation of the unit can be expected when the ratio of static to dynamic pressure is at least 10 to 1. From Figure 19, it can be seen that this occurs when the needle-bead distance is less than one-tenth of the needle diameter.

In the actual amplifier units, with a needle diameter of .020", this average distance is .002", that is to say, the force balance postulated in our mathematical analysis occurs when the bead-needle distance is within those two-thousandths of an inch. For successful operation, the bead should never touch the needle since these mechanical forces will affect the force balance but not appear on the output. This is extremely difficult to achieve for the required average clearances discussed above. The needle tip may have some irregularities, the needle may not be perfectly installed, but even more important, the asymmetric deformation of the bead due to gravity and the basic instability between the liquid surface and the needle tip make it impossible to avoid direct contact between the fluid bead and the needle for extremely close ranges of operation. This instability results from the mobility of the fluid surface.* If the needle tip plane and the liquid surface are not absolutely parallel, changes in the resulting gas flow pattern tend to increase the angle; this continues until the liquid surface touches one side of the needle tip and the gas escapes through the other side.

---

*This was suggested by Professor F. Ezekiel, consultant to NASA Electronics Research Center.

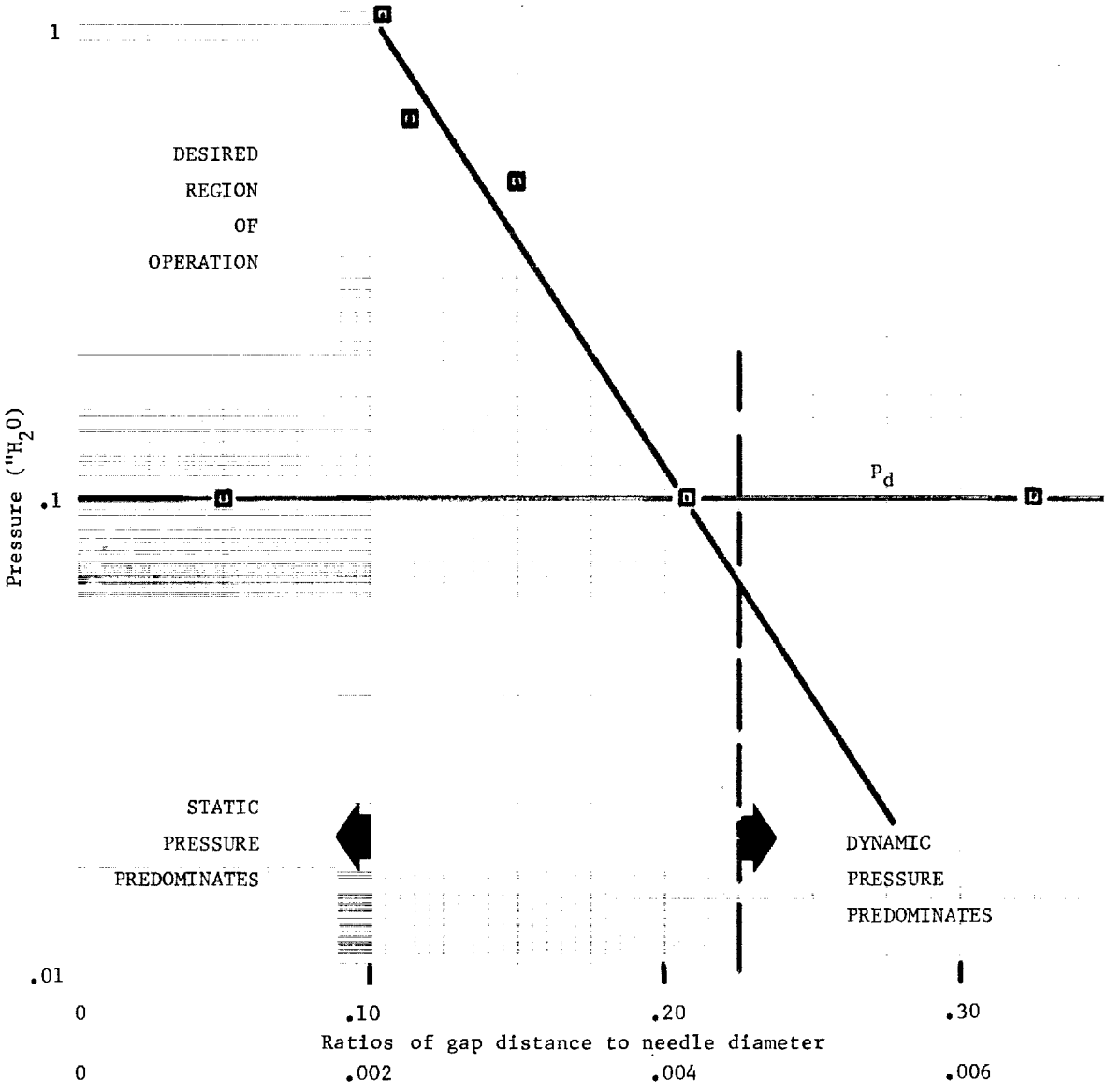

FIGURE 19 Static-Dynamic Pressure Relationship
(Bead Pressure Distribution)

Experiments obtained by placing the units vertically so that gravity has a symmetric effect on the bead, show that the gravity effect is relatively small. Therefore, it may be concluded that the instability of the bead surface against the needle flow is the basic reason why the gain amplifier units cannot operate successfully at high gains.

Friction Experiments

The gain amplifier units show hysteresis effects in various degrees. However, the buffer amplifier units were much less sensitive to these effects. The gain amplifier units exhibit a high level of hysteresis due to friction that decreases after the device has been in operation for some time. Friction effects are more apparent in the gain units because in order to overcome friction and to provide a balance to the applied control pressure, the pressure in the output circuit has to increase substantially. This is a result of the output pressure acting over a small effective area in these units.

Therefore, friction effects are negligible in units where the output pressure acts upon the whole face of the bead (such as in the buffer configurations), but may show up strongly in those configurations where the balancing pressure acts over a limited area of the bead.

The mechanism that produces resistance to the motion of the bead is not clear; however, there are some indications as to its nature. Ideally, the motion of a liquid bead in a polished chamber should be almost frictionless, even if non-slip conditions at the wall are assumed. This would only create a viscous type of friction which would not be apparent at the low velocities encountered during static testing.

Another possible source of friction is the work done in generating a new molecular "skin" at the leading edge of the bead. This is necessarily a direct result of assuming non-slip at the wall. Then the surface of the bead behaves as a tank or tractor tread. As the bead moves forward, an axisymmetric flow is induced. A new surface would be generated at the central portion of the leading bead meniscus and the same amount of surface would be absorbed at the trailing meniscus.

For this effect to result in a finite drag on the bead, the work done in generating the surface has to be larger than the work produced in collapsing it later on. Although it is difficult to evaluate this mechanism, the basic concept can be applied to an actual skin covering the bead.

When a fresh mercury bead is exposed to air, an oxide film is formed on the surface in a matter of minutes. This film has been observed under the microscope during the operation on the amplifiers. It is believed that the oxide film is the main source of friction in a mercury bead. This suggests that when mercury is to be used for experiments, special precautions must be taken to minimize chemical activity on its surface. These precautions might include the use of inert atmospheres such as helium, or of coating substances, such as silicon oils.

A series of experiments was carried out to measure the level of friction on a mercury bead in a Plexiglas chamber. The force required for incipient motion was obtained by tilting the chamber and measuring the angle necessary to move the bead. Measurements were also taken of the pressure required for incipient motion in a level chamber. These two types of measurements gave consistent results.

Experiments carried out in chambers of different diameters showed that the smaller the diameter, the higher the friction.

The friction levels, when expressed in terms of a friction factor (using the weight of the bead as the normal force) yielded values of about .15 on the average.

Design Optimization

Although the optimization process was not a formal one, certain aspects investigated will be presented here.

Bead dynamics.--In equation (38) of the mathematical analysis, the natural frequency of the bead is given as:

$$\omega_n = \sqrt{\frac{2K}{M}}$$

but $$K = \frac{\gamma p A}{x_o} \quad \text{and} \quad M = \rho \ell A \ .$$

Therefore, $$\omega_n = \sqrt{\frac{nP}{\rho \ell x_o}} \tag{44}$$

where:

- P is operating pressure
- ρ is bead density
- ℓ is length of bead
- x_o is length of air space

Thus, to maximize natural frequency we must:

1. use maximum operating pressure;
2. select liquid with low density;
3. keep length of bead short; and
4. minimize length of air space.

Note that the cross-sectional area of the chamber is not a factor in the natural frequency. Therefore, fast amplifiers can be designed to any size for which suitable liquids are available.

Chamber size.--The chamber diameter has an upper bound controlled by the surface tension of the liquid. If the chamber is bigger than .130" for mercury, the bead will not "stick" to the top portion of the tube and the proper sealing will not be achieved.

The minimum chamber size is determined by the allowable level of friction The friction experiments above showed that chamber diameters below .060" do not work well. The best size was found to be between .075" and .095" in diameter.

Needle size.--In the buffer configurations, the gas flows from the chamber out through the needle. This produces a tendency to push or extrude the bead into the needle. Thus, for buffer-type amplifiers using a mercury bead, a .010" I.D. needle was found to be the optimum size.

On the other hand, in the case of a gain-type amplifier, the jet issuing from a small-diameter (less than .020") needle tends to puncture the bead. If the needle diameter is too large (larger than .040"), it becomes difficult to match the needle tip to the bead surface. The size used in the final prototypes was .020" diameter.

Needle geometry.--In the course of examining the various possible configurations, a number of needle geometries were tested. Beveled needles were tried to match the tip plane to the bead surface; a tapered needle was also fabricated to decrease the fixed needle resistance versus the variable resistance. A concentric needle was used to attempt to improve the pressure distribution on the bead and to decrease bead surface deformation. None of these needles showed a decided improvement over the straight needle.

CONCLUSIONS

1. It has been shown that it is feasible to build a useful infinite-input-impedance amplifier using the two-phase fluidic concept.

2. Three configurations are possible: the buffer (one-to-one) amplifier, the gain amplifier, and the buffer-gain type.

3. Of these three types, the gain amplifier shows substantial hysteresis effect due to friction when a mercury bead is used. Friction appears to be negligible in the other two types.

4. Actual gains up to 5 can be achieved in the gain amplifier. The buffer-gain type has been tested at gains of about 10, with a potential for higher levels.

5. In order to achieve the high gains required for operational amplifier use, two or more amplifiers will have to be cascaded.

6. Dynamic analysis has shown that by judicious design, the two-phase amplifier can be made to behave dynamically as a first-order system. Optimization for dynamic response has not been fully investigated.

7. The bandwidth of some of the units tested was higher than 50 hertz.

8. Preliminary investigation shows that several non-toxic chemical systems have most of the physical characteristics necessary to replace mercury in the analog amplifier.

9. Static and dynamic test results indicate that it is possible to construct analog computer circuitry with the buffer and buffer-gain configurations. A flat response up to 50 hertz seems adequate for many computing applications.

RECOMMENDATIONS

1. Further effort should be devoted to testing substitute chemical systems in the prototype amplifier designs.

2. The search for other chemical systems to replace mercury should be continued.

3. Further effort should be devoted to optimizing amplifier designs for dynamic response and resistance to environment.

4. The buffer amplifier is at a state of development where evaluation in computing circuits is the next logical step. It is recommended that analog operational amplifier circuits of known or predictable response be constructed. This will allow the evaluation of the amplifier as a computational component.

APPENDIX A -- NEW TECHNOLOGY

"After a diligent review of the work performed under this contract, no new innovation, discovery, improvement or invention was made."